

Analysis of adaptive walks on NK fitness landscapes with different interaction schemes

Stefan Nowak and Joachim Krug

Institute for Theoretical Physics, University of Cologne, Cologne, Germany

E-mail: sn@thp.uni-koeln.de, krug@thp.uni-koeln.de

Abstract. Fitness landscapes are genotype to fitness mappings commonly used in evolutionary biology and computer science which are closely related to spin glass models. In this paper, we study the NK model for fitness landscapes where the interaction scheme between genes can be explicitly defined. The focus is on how this scheme influences the overall shape of the landscape. Our main tool for the analysis are adaptive walks, an idealized dynamics by which the population moves uphill in fitness and terminates at a local fitness maximum. We use three different types of walks and investigate how their length (the number of steps required to reach a local peak) and height (the fitness at the endpoint of the walk) depend on the dimensionality and structure of the landscape. We find that the distribution of local maxima over the landscape is particularly sensitive to the choice of interaction pattern. Most quantities that we measure are simply correlated to the rank of the scheme, which is equal to the number of nonzero coefficients in the expansion of the fitness landscape in terms of Walsh functions.

Submitted to: *J. Stat. Mech.*

1. Introduction

In evolutionary biology, adaptation is the process by which the genetic structure of a population changes in response to its environment. This process relies on two basic requirements: The supply of new individuals that differ from the prevalent ones, and the selection of individuals that have some kind of advantage over the others. Differences between individuals can be ascribed to differences in their genetic blueprint, the DNA, that are caused, e.g., by mutation, and the advantage that is relevant for selection is an increased number of offspring that the better adapted individuals leave in the next generation. Instead of using four-lettered DNA sequences, the genotype is often represented as a binary sequence of length L . Its letters, usually taken to be 0 and 1, are then interpreted as two different alleles that can be present at a genetic locus. The set of genotypes has the structure of a hypercube, a graph with nodes corresponding to sequences and edges connecting two sequences when they differ by a point mutation in a single letter. Assuming that the genotype fully specifies the reproductive success of an individual, one may envision a mapping from the space of genotypes to the number of offspring or some related fitness measure. Such a mapping is called a fitness landscape [1, 2, 3].

Mutations modify the genotype by changing a certain letter from zero to one or vice versa. Whenever a new mutation arises it may become fixed, which means that it is carried by all individuals in the population. The chance for this event increases with the fitness of the new genotype compared to the average fitness of the population [4, 5]. If the fitness decreases due to mutation, fixation can only happen by stochastic fluctuations [6]. As the strength of these fluctuations decreases with population size, for large populations a mutant can survive only if its fitness is larger than average. When additionally the rate of supply of new mutants is low such that the timescale of fixation is much smaller than the typical time between the appearance of different mutants, the population is monomorphic most of the time. In this regime of strong selection and weak mutation [7, 8] the dynamics can be approximated as an adaptive walk, in which the whole population is treated as a single entity that travels uphill in the fitness landscape by single mutational steps. Since the fitness has to increase in each step, these walks terminate when there is no neighboring genotype with larger fitness available, i.e., when a local fitness maximum has been reached.

The structure of the underlying fitness landscape is crucial for population dynamics like adaptive walks and is often characterized in terms of its “ruggedness” which can be measured, for instance, by the number of local maxima [2, 3]. Though there exist an increasing number of empirical fitness landscapes for small sequence lengths L [2, 3, 9, 10, 11, 12, 13, 14, 15], the mechanism by which a genotype affects the fitness is exceedingly complex, and therefore probabilistic models are often used for theoretical studies. In the simplest case, the fitness values are assigned independently to each genotype from some probability distribution, a setting referred to as the House of Cards (HoC) model [16, 17].

A more sophisticated model for fitness landscapes is the NK model [18, 19], which is based on the following idea: The total fitness of a genotype is the sum of several different contributions that are related to different properties of the individual and depend on different parts of the genotype. How large these parts are is controlled by the parameter K , while N specifies the sequence length in standard notation and hence the name of the model (note however that we will use L instead of N , as the latter is often reserved for the population size). Different parts may, and usually do, overlap and therefore one gene influences several contributions to the total fitness. The pattern into which the genotype is sectioned specifies the scheme of interaction between genes, also known as the genetic neighborhood.

Fitness landscapes in general and the NK model in particular are also relevant to fields outside of biology. In physics, the concept of an energy landscape is very similar to that of a fitness landscape [20]. While a population evolves into a state with high fitness, physical systems are driven to states of low energy. Binary sequences in particular can naturally be interpreted as the configuration of a system with interacting spins. In this context the HoC model is the analogue of Derrida's random energy model [21], while the NK model can be interpreted as a superposition of diluted p -spin glass models [22]. In computer science, the NK model is used as a benchmark for optimization but especially as an example for an NP-complete problem [23, 24, 25, 26].

Among the large number of studies on the NK model (e.g., [18, 27, 24, 28, 29, 30, 31, 32, 33, 34, 35], see also section 2.2), only few have explicitly addressed how the choice of the interaction scheme affects the properties of the landscapes [36, 37]. The answer to this question turns out to depend strongly on the quantity under consideration. On the one hand, despite earlier claims to the contrary [38], the fitness autocorrelation function is manifestly independent of the interaction scheme [39, 40]. On the other hand, the accessibility of the global fitness maximum along paths of monotonically increasing fitness is highly sensitive to the structure of the genetic neighborhood [34, 36].

The goal of this article is to systematically study the influence of different genetic interaction schemes on the landscape. Our main tool for the analysis are adaptive walk, for two reasons. First, despite their simplicity adaptive walks represent a biologically relevant limit of population dynamics and are commonly used for the interpretation of microbial evolution experiments [41]. Second, and most importantly, adaptive walks allow for the numerical study of rather large landscapes. Keeping in mind that a landscape consists of 2^L genotypes, it is impossible to keep track of all of them when the genotype size L becomes large. Even the study of local maxima, which does not necessarily require the knowledge of the entire landscape, becomes infeasible quickly since their relative frequency decreases exponentially with L [28, 29, 30]. Adaptive walks, on the other hand, find local maxima rather fast, require only a tiny fraction of the landscape to be known and are still strongly influenced by the overall shape of the landscape, i.e., they conveniently translate global properties of the landscape into local ones.

The article is structured as follows: In section 2 we provide the mathematical

framework and discuss the models for fitness landscapes and adaptive walks in more detail. The results can be found in section 3 which is divided into three parts. In section 3.1 we study a specific interaction scheme that enables us to derive several quantities of interest analytically, which subsequently serve as a point of comparison to other genetic neighborhood types. In section 3.2 we examine numerically the neighborhood types that are most common in the literature, and in section 3.3 we discuss the clustering of local maxima. We then introduce the rank of an interaction scheme [37] as a possible quantification of neighborhood types in section 3.4 and show that most landscape properties are correlated with it. Finally, the results are summarized and discussed in section 4.

2. Models and methods

2.1. Space of genotypes and fitness landscapes

In general, a genotype can be represented by a sequence of L letters that are drawn from an alphabet of a specific size. Here we will assume a binary alphabet for simplicity, i.e., each genotype $\sigma = (\sigma_1, \dots, \sigma_L)$ is an element of $\{0, 1\}^L$. Together with the Hamming distance

$$d(\sigma, \tau) = \sum_{i=1}^L (1 - \delta_{\sigma_i \tau_i}) \quad (1)$$

this can be extended to a metric space, the hypercube \mathbb{H}_2^L . The distance $d(\sigma, \tau)$ is the minimal number of mutations required to change the genotype from σ to τ (or vice versa). A succession

$$\Sigma = \sigma^1 \rightarrow \sigma^2 \rightarrow \dots \rightarrow \sigma^n \quad (2)$$

of genotypes is called a path, if $d(\sigma^i, \sigma^{i+1}) = 1$ for all i .

In order to quantify the reproductive value of a certain genotype σ a fitness values $F(\sigma) \in \mathbb{R}$ is assigned to each sequence. This mapping is called a fitness landscape. The fitness is a measure of how well the organism is adapted to its environment, and can be related to the (mean) number of offspring an individual with the corresponding genotype will leave in the next generation. A mutation from σ to τ is called beneficial if $F(\tau) > F(\sigma)$, and deleterious if $F(\tau) < F(\sigma)$. Due to natural selection, only beneficial mutations can become prevalent in large populations. Therefore a population undergoing adaptation propagates through the space of genotypes along a path of monotonically increasing fitness. Such a path, where $F(\sigma^{i+1}) > F(\sigma^i)$ for all i , is called accessible [9, 10, 42, 34, 43].

Commonly used probabilistic models for fitness landscapes are the House-of-Cards (HoC) model, the Rough-Mount-Fuji (RMF) model [42, 44, 45] and the NK model. Out of these three, the HoC model is the simplest as the fitness values $F(\sigma)$ are assigned independently to each genotype σ from some probability distribution. For the HoC model, the number of maxima is particularly easy to calculate [17]: A sequence σ is a

local maximum if and only if its fitness is larger than that of all of its neighbors, i.e., if it is the largest of $L + 1$ random variables. The probability for this is $1/(L + 1)$ and there are 2^L genotypes in the landscape, hence the expected number of maxima is $2^L/(L + 1)$.

2.2. The NK fitness landscapes

The NK-model introduces correlations between the fitness values of different genotypes. In this model, the fitness $F(\sigma)$ of a sequence σ is given by

$$F(\sigma) = \sum_{i=1}^L f_i(\sigma_{b_{i,1}}, \sigma_{b_{i,2}}, \dots, \sigma_{b_{i,K}}) \quad (3)$$

where the f_i are independent HoC landscapes of size K , i.e., the $f_i(\sigma)$ are random numbers drawn independently from the same distribution for each i and each $\sigma \in \{0, 1\}^K$, such that a total of $L2^K$ random numbers are required for generating one realization of the landscape. Unless mentioned otherwise, we will use f_i drawn from a standard normal distribution throughout this article, i.e., the marginal fitness of a specific genotype is normally distributed with zero mean and variance L .

The $b_{i,j}$ determine the interaction between genetic loci. For some purposes, it is more convenient to express the interaction matrix $b_{i,j}$ in terms of neighborhood sets

$$V_i = \{b_{i,1}, b_{i,2}, \dots, b_{i,K}\}. \quad (4)$$

From a biological viewpoint there are no obvious constraints on the structure of the interaction sets, but in the NK literature it is usually assumed that the number of sets is equal to the sequence length L , that all sets contain the same number K of elements, and that $i \in V_i$ for all i . The parameter K is interpreted as a ruggedness parameter and interpolates from a purely additive landscape with a single maximum ($K = 1$) to the maximally rugged HoC landscape ($K = L$). Note that we use K to denote the total number of elements in an interaction set. This is slightly different from the usual definition, where K is the number of elements in addition to i , and hence in our notation K is increased by 1 compared to the standard notation.

The most common types of neighborhoods, which we are also going to use in this article, are the following (see figure 1 for illustration).

Adjacent neighborhood: Each sub-landscape f_i depends on the i -th locus and its $K - 1$ neighbors. The neighborhood sets are given by

$$V_i = \{i, i + 1, \dots, i + K - 1\}, \quad (5)$$

each element modulo L .

Random neighborhood: The neighborhood set V_i contains i and $(K - 1)$ other numbers, which are chosen at random from $\{1, 2, \dots, L\}$.

Block neighborhood: The neighborhood sets are given by

$$V_i = \{\lceil i/K \rceil, \lceil i/K \rceil + 1, \lceil i/K \rceil + K - 1\} \quad (6)$$

where $\lceil x \rceil$ is the ceiling function. This means that K consecutive sets are equal, dividing the genotype into L/K independent blocks (L should be an integer multiple of K here). Each block is a HoC landscape.

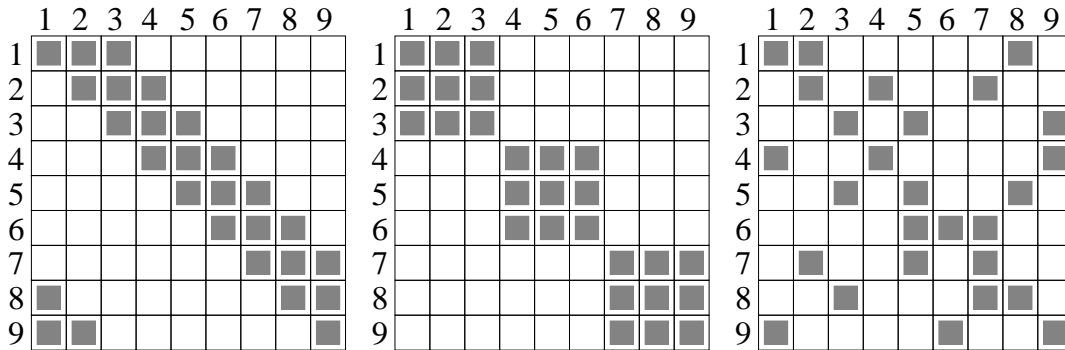


Figure 1. Illustration of the standard neighborhoods for $L = 9$ and $K = 3$. From left to right: Adjacent, block, and random neighborhood. A grey square in row i and column j means that V_i contains j .

Compared to the HoC model, little is known analytically about the NK model, except for some special cases. One example, apart from the additive case $K = 1$ and the HoC case $K = L$, is the model with block neighborhood which facilitates analytical approaches due to its modular structure [27, 32]. As a consequence, properties like the number of maxima or the number of accessible paths to the global maximum can be derived from results for the HoC model [27, 36]. A detailed analysis of the NK model with adjacent and random neighborhoods was carried out by Weinberger [46], who derived approximate asymptotic expressions for the number and fitness values of local maxima as well as for the mean length of adaptive walks. In accordance with much of the early literature on the NK-model (e.g., [19]), Weinberger concluded that these quantities are the same for the adjacent and random neighborhoods or at least that differences between the two schemes are minor.

A rigorous result for the adjacent neighborhood model is that the mean number of maxima grows asymptotically as $(2\lambda_K)^L$ with a constant λ_K that increases with K and depends in general on the underlying fitness distribution of the sub-landscapes f_i [29]. The constant is known exactly for a few distributions and specific, small values of K . For the exponential distribution, $\lambda_2 \approx 0.5627$ and $\lambda_3 \approx 0.6114$, for a gamma distribution with shape parameter 2 one finds $\lambda_2 \approx 0.5646$ [28], and for a negative exponential distribution $\lambda_2 \approx 0.5770$ [29]. In Appendix B we present a rather straightforward calculation to show that

$$\lambda_2 = \frac{1}{6} \left[3 - \sqrt{3} + \sqrt{6(\sqrt{3} - 1)} \right] \approx 0.5606$$

for a gamma distribution with shape parameter $1/2$. For large K and arbitrary distributions it has been conjectured, that λ_K grows asymptotically as $\exp[-\log(K)/K]$, but this was proven only for Gaussian and fat-tailed distributions [30].

2.3. Fourier decomposition of fitness landscapes

Any fitness function $F(\sigma)$ on the hypercube \mathbb{H}_2^L can be expanded into eigenfunctions of the corresponding graph Laplacian [22, 35, 47]. The resulting transformation is a discrete analogue of the Fourier transform [48] and also known as the Walsh transform in computer science [25, 49]. It takes on a particularly simple form if the binary genotypes are represented by sequences $s \in \{-1, 1\}^L$ which can be interpreted as configurations of a spin system. In this representation, the eigenfunctions of order p are proportional to products $s_{i_1} s_{i_2} \dots s_{i_p}$ where $0 \leq p \leq L$ and the indices i_1, i_2, \dots, i_p are a subset of $\{1, 2, \dots, L\}$. For the NK-model the expansion terminates at order $p = K$, and hence any NK fitness landscape can be written as

$$F(s) = F_0 + \sum_{i=1}^L H_i s_i + \sum_{p=2}^K \sum_{i_1 \dots i_p} J_{i_1 \dots i_p} s_{i_1} \dots s_{i_p} \quad (7)$$

where the random “magnetic fields” H_i and the “coupling constants” $J_{i_1 \dots i_p}$ are determined by the original set of random functions f_i . In most cases, the coefficients are extremely sparse as a particular coupling constants $J_{i_1 \dots i_p}$ is nonzero only if there is at least one neighborhood set V such that $i_j \in V$ for all $j \in \{1, \dots, p\}$. The number of nonzero coefficients is called the *rank* of the landscape [37] and will be used to characterize different neighborhood types below in section 3.4.

The Fourier spectrum of a fitness landscape is obtained from the Fourier expansion by summing the squared coefficients of a given order p . Suitably normalized, this provides a measure for the weight of genetic interactions of different orders, and thus a quantification of the ruggedness of the landscape [2, 3, 49]. The Fourier spectrum is related to the fitness autocorrelation function through a one-dimensional linear transformation involving discrete orthogonal polynomials [22]. For the NK-model the Fourier spectrum, like the fitness autocorrelation function, is independent of the genetic interaction scheme and can be explicitly calculated [35]. In contrast, as we will see in section 3.4, the rank depends strongly on the choice of the genetic neighborhood.

2.4. Adaptive walks

An adaptive walk (AW) is an idealized evolutionary process. Rather than treating the population as a set of individuals, it behaves like a single entity that travels through the genotype space. Formally an AW is a Markov chain on \mathbb{H}_2^L with dynamics defined by transition probabilities $p(\sigma \rightarrow \tau)$ for a step from genotype σ to τ . Such a step is allowed only if τ can be reached from σ by a single beneficial mutation, i.e., if $d(\sigma, \tau) = 1$ and $F(\sigma) < F(\tau)$; otherwise $p(\sigma \rightarrow \tau)$ is zero. This means that all paths generated by an AW are accessible. The walk terminates on some genotype σ if no further beneficial mutations are possible, i.e., when σ is a local fitness maximum. The number of steps to the maximum will be called the length ℓ of the AW and the fitness at the maximum will be called its height h .

Concerning the probabilities of allowed steps, we distinguish between different kinds of adaptive walks.

Natural AW: The transition probabilities have the fitness dependent values

$$p(\sigma \rightarrow \tau) = \frac{F(\tau) - F(\sigma)}{\sum_{\sigma'} [F(\sigma') - F(\sigma)]}, \quad (8)$$

where the sum runs over all fitter neighbors σ' of σ .

Random AW: Each step leads to a randomly chosen fitter neighbor.

Greedy AW: Each step leads to the fittest available neighbor.

Reluctant AW: A step is always taken to the least fit neighbor that is still fitter than the current genotype.

Note that the dynamics of greedy and reluctant walks is completely deterministic on a given realization of the landscape. The dynamics of the natural AW is the most realistic, in the sense that it can be derived from individual based population models like the Wright-Fisher or Moran model [7, 8, 50, 51]. We will however not treat this walk type here because its dynamics is influenced by the distribution of fitness values [52, 53]. This is in contrast to the other walk types, where the behavior does not depend on the actual fitness values but only on their order. Greedy and random AWs can be interpreted as limits of more general and realistic dynamics [54], and at least for the HoC landscape natural AW's interpolate between them in terms of length [8]. The reluctant walk does not seem to have a biological interpretation and therefore has not been considered previously in the biological literature, but it appears in the context of spin glasses and optimization [55, 56, 57, 58]. We will use it here as an additional tool for the analysis of fitness landscapes.

A number of results are available for random and greedy AW's on the HoC landscape. For $L \gg 1$, the mean length of a random AW is given by $\ell_{\text{HoC}}^{\text{rnd}} \approx \ln L$ [17, 59, 60, 61], while the length of the greedy AW attains a constant limiting value $\ell_{\text{HoC}}^{\text{grd}} = e - 1 \approx 1.7183$ [62]. Using the results of [61, 62], in Appendix A.1 and Appendix A.2 we derive the mean value of the walk height for random and greedy AW's in the HoC landscape. Assuming without loss of generality that the fitness values are uniformly distributed on the interval $[0, 1]$, the mean height is of the form $\langle h \rangle = 1 - \alpha/L$ to leading order, where α is a constant depending on the walk type. To our knowledge, no rigorous results are available for the reluctant walk, but numerically it turns out that its mean length is given by $\ell_{\text{HoC}}^{\text{rel}} = L/2$ and the height constant is $\alpha = 1$ (see Appendix A.3). A summary of the mean walk lengths and heights can be found in table 1. The fact that $\alpha = 1$ for the reluctant AW implies that the maxima found by this dynamics are typical local maxima, whereas the random and greedy walks for which $\alpha < 1$ find exceptionally high peaks. Moreover, on the HoC landscape the greedy AW reaches higher fitness levels than the random AW.

Table 1. Properties of adaptive walks on the House-of-Cards landscape with uniformly distributed fitness values. The derivation and exact values of α can be found in Appendix A. The results for the reluctant walk were obtained numerically.

Walk type	Length $\langle \ell \rangle$	Height $\langle h \rangle = 1 - \alpha/L$
Greedy	$e - 1$	$\alpha = 0.4003\dots$
Random	$\log L$	$\alpha = 0.6243\dots$
Reluctant	$L/2$	$\alpha = 1$

3. Results

3.1. Exact results for the block model

In the block model, each path can be decomposed into sub-paths, where each sub-path is confined to one specific block [27, 36]. For example, for $L = 4$ and $K = 2$, the path

$$\Sigma = (0011) \rightarrow (1011) \rightarrow (1001) \rightarrow (1000) \rightarrow (1100)$$

can be decomposed into $\Sigma^1 = (00) \rightarrow (10) \rightarrow (11)$ in the first block and $\Sigma^2 = (11) \rightarrow (01) \rightarrow (00)$ in the second one. The first mutation occurs in block 1, the second and third mutation in block 2 and the fourth one again in block 1, but note that any other order would also lead to a valid path with the same endpoint. This means that, in order to construct the full path Σ from the Σ^i , one also needs to know the order $\underline{\pi}(\Sigma)$ in which the blocks are affected [36]. However, this order has no influence on the final genotype, the length of the path or its accessibility.

One can easily show that the probability of an adaptive step $\sigma \rightarrow \tau$ in the full landscape, conditioned on taking place in block b , is equal to the probability of the corresponding step in the sub-landscape of that block. This is true under the fairly general condition that the transition probabilities depend only on fitness differences, which applies to all adaptive walk types defined in section 2.4. Hence the probability that a path Σ is taken in an adaptive walk is given by

$$\mathbb{P}(\Sigma, \mathcal{L}) = \mathbb{P}(\underline{\pi}(\Sigma), \mathcal{L}) \prod_{i=1}^{L/K} \mathbb{P}(\Sigma^i, \mathcal{L}^i), \quad (9)$$

where $\mathbb{P}(\Sigma, \mathcal{L})$ is the probability of taking path Σ in landscape \mathcal{L} , \mathcal{L} is the full landscape, \mathcal{L}^i is the sub-landscape of block i and $\mathbb{P}(\underline{\pi}(\Sigma), \mathcal{L})$ is the probability for treating the blocks in the specific order $\underline{\pi}(\Sigma)$.

As the order of blocks has no influence on the statistics we are interested in, namely the length and height of an adaptive walk, one can treat a walk in the full landscape simply as the succession of independent walks through the sub-landscapes. More precisely, if ℓ_i denotes the random variable which represents the length of the walk in block i , the length of the full walk is given by $\ell = \sum_i \ell_i$. In the standard block model,

the mean walk length is accordingly given by

$$\langle \ell \rangle = \sum_{i=1}^{L/K} \langle \ell_i \rangle = \frac{L}{K} \langle \ell_1 \rangle = \frac{L}{K} \ell_{\text{HoC}}(K). \quad (10)$$

For a random AW this leads for instance to $\ell_{\text{NK}}^{\text{rnd}} \approx \frac{L}{K} \log K$. This result was already obtained by Weinberger from an analysis of the density of local maxima [46], but appeared there as an approximation for adjacent and random neighborhoods rather than as an asymptotically exact statement for the block model. Interestingly, according to this argument the mean length of reluctant walks is given by $\langle \ell \rangle = L/2$ and does not even depend on K . In practice, the usefulness of the relation (10) relies on an accurate knowledge of mean walk lengths on the HoC landscape. Since the analytical expressions in table 1 are only valid asymptotically for large K , we include a small- K correction to $\ell_{\text{HoC}}(K)$ that consists of two additional terms proportional to $1/K$ and $1/K^2$ with coefficients obtained by a least square fit to simulation data.

The same argument as for the length can be used to estimate the height of an adaptive walk. We have

$$h = \sum_{i=1}^{L/K} h_i, \quad (11)$$

where h is the height in the full landscape and h_i the height in the i -th block. Since the h_i have the same statistics as walk heights in the HoC model, one can compute the mean of h with the help of previous results. Using additivity of the mean value as well as equation (A.30) derived in Appendix A.2, we obtain

$$\langle h \rangle = \frac{L}{K} \langle h_1 \rangle \approx \frac{L}{K} Q^{-1} \left(1 - \frac{\alpha e^{-\gamma}}{K} \right), \quad (12)$$

where Q is the CDF within a block, $\gamma \approx 0.5772$ is the Euler-Mascheroni constant and α depends on the walk type (see table 1). Note that the second approximation is only valid for fitness distributions from the Gumbel class of extreme value theory [63] and is applied here for a normal distribution with zero mean and variance K .

3.2. Comparison of standard neighborhood types

In the block neighborhood, both mean length $\langle \ell \rangle$ and height $\langle h \rangle$ of AW's are linear in the sequence length L (if K is fixed), as can be trivially seen from (10) and (12). Strictly speaking, this is not true for the other neighborhood types, since the genetic sequences cannot be divided into independent blocks anymore. However, as shown in figure 2, for $L \gg K$ the linear behavior approximately applies for all interaction schemes. When L is comparable to K the linear behavior only changes slightly, which leads to a linear regression with almost vanishing intercept. A notable exception is the reluctant walk on a landscape with random neighborhoods, where the intercept is negative and very large compared to the slope [inset of figure 2(a)].

The slope of the linear L -dependence of $\langle \ell \rangle$ and $\langle h \rangle$ in figure 2 differs markedly between different neighborhood and walk types. As in the HoC model, the greedy walk

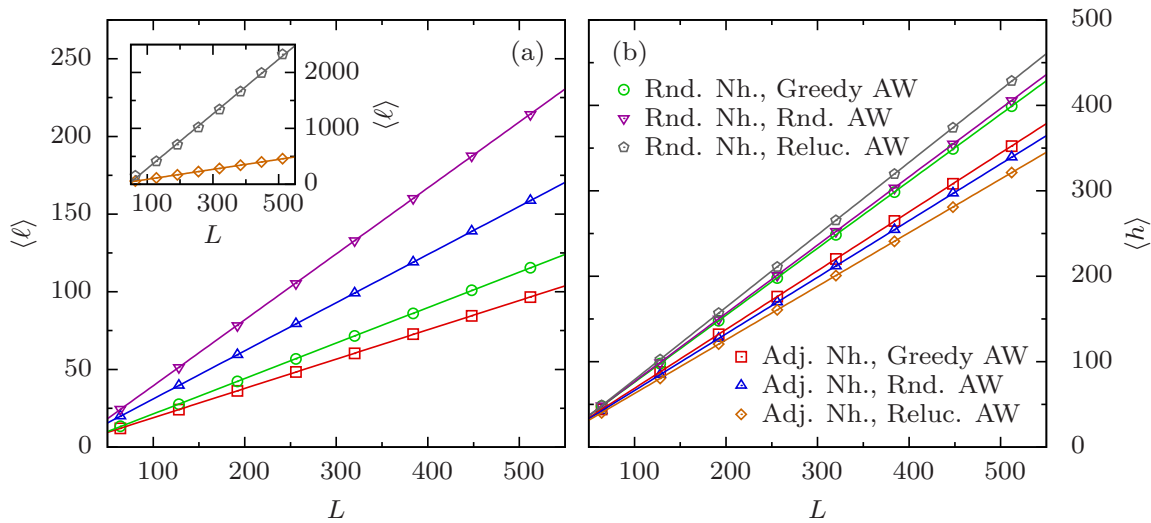


Figure 2. Adaptive walk length (a) and height (b) for the NK model with fixed $K = 8$ and varying L . The symbols used for the different walk and neighborhood types are explained in panel (b). Lines correspond to linear regressions.

has the shortest length of all the walk types, the reluctant walk is the longest and random adaptive walks are in between. The neighborhood type has an influence on the length which is comparable in strength to that of the walk type. For a given walk type, random neighborhoods facilitate longer walks than adjacent neighborhoods, which in turn give rise to longer walks than the block neighborhood. The influence of the neighborhood on walk length is most pronounced for the reluctant walk [see the inset of figure 2(a)]. The ordering of neighborhood types remains the same if one looks at the walk height instead of length, but the situation regarding the different walk types is more complex [figure 2(b)]. While for the adjacent and block neighborhood the height increases with the “greed” of the walk, the order is reversed for the random neighborhood. However, this is not the case in general but only for suitable choices of K (see also figure 4).

Both lengths and heights of AW’s depend sensitively on K , with the length of reluctant walks in the block model being the only exception. Figure 3 shows the dependence on K for different choices of the neighborhood and walk type. For all values of K (except $K = 1$ and $K = L$) both walk length and height are consistently largest with random neighborhood, second largest with adjacent neighborhood and smallest with block neighborhood. The difference between neighborhood types is most apparent for intermediate values of K . This is not surprising, because for $K = 1$ and $K = L$ all neighborhood types are equivalent and the behavior is expected to change smoothly with K .

Since the local maxima of the fitness landscape are the absorbing states for adaptive walks, their number N_{\max} should be inversely correlated with the length of adaptive walks. In agreement with other studies [36, 37], our findings thus suggest that, for given values of L and K , N_{\max} is largest in a landscape with block neighborhood, slightly

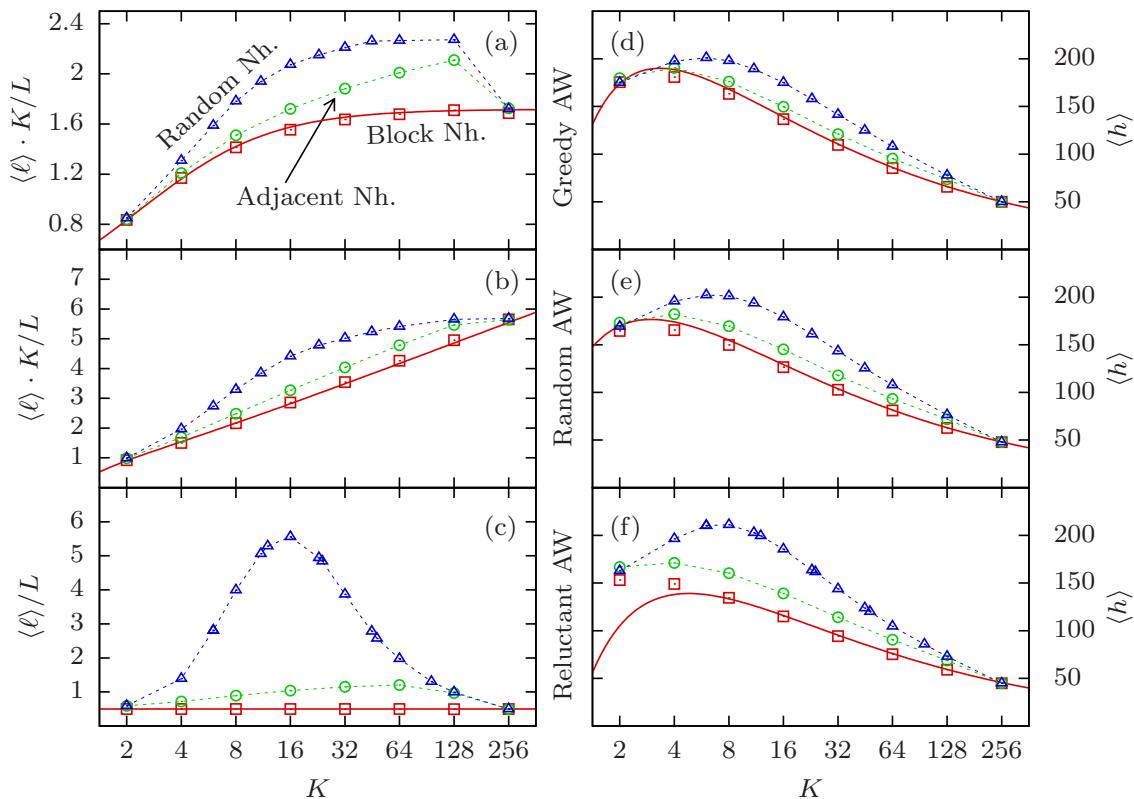


Figure 3. Adaptive walk length (a)-(c) and height (d)-(e) for the NK model with fixed $L = 256$ and varying K . Note that different scalings of the mean lengths $\langle \ell \rangle$ have been applied in panels (a)-(c) in order to emphasize the differences between neighborhood types. Solid lines correspond to the analytical expressions for the block neighborhood given by (10) and (12), respectively. Symbols are explained in panel (a), and dashed lines are for visual guidance.

decreased for adjacent neighborhood and the smallest for random neighborhoods. Moreover, assuming that the number of maxima generally increases with K , this should result in a decrease of $\langle \ell \rangle$ which can indeed be observed for greedy and random AWs (but note that this is not visible in figure 3 because of the scaling of $\langle \ell \rangle$). However, reluctant walks show an unexpected departure from this pattern. The reluctant walk length is constant in K in the block model and displays a non-monotonic behavior for adjacent and random neighborhoods [figure 3(c)]. In particular, the combination of the reluctant walk and random neighborhoods results in extremely long walks with a length that is several times larger than the diameter L of the genotype space. This implies that on average each site in the sequence mutates several times before a local maximum is reached.

Similarly, the height of adaptive walks should be related to the height of local maxima. In previous work it was found that the height of an average local maximum in the NK-model decreases asymptotically as $\sqrt{\log(K)/K}$ for large K [29, 46]. The relevance of this effect in the present context should however not be overestimated,

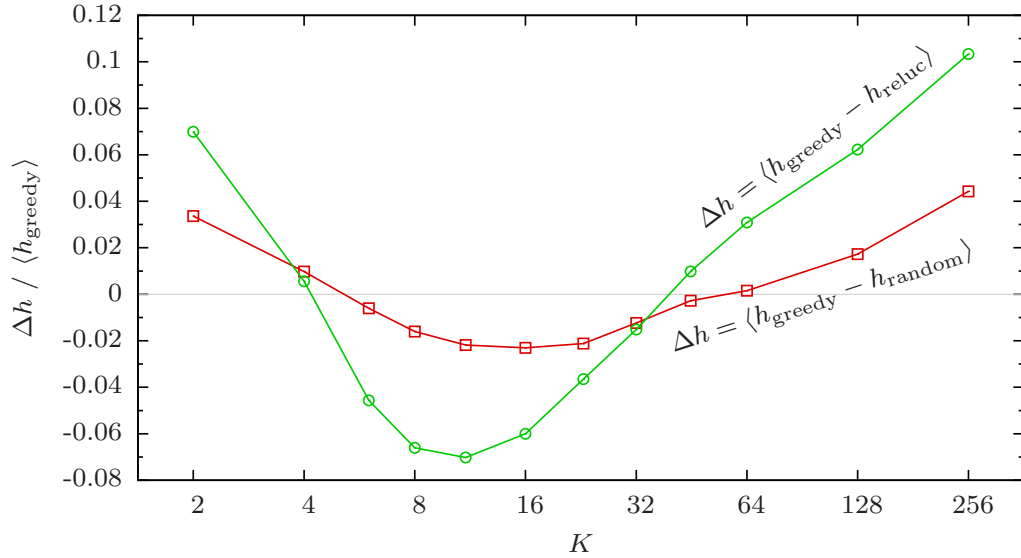


Figure 4. Differences in walk height for an $L = 256$ landscape with random neighborhood. Lines are for visual guidance.

since the results described in section 2.4 for the HoC landscape show that adaptive walks generally do not terminate on random maxima but on particularly high ones. As more maxima become available with increasing K , the walks might find higher ones even though their average height decreases. Be that as it may, the resulting dependence of $\langle h \rangle$ on K is not monotonic and has a maximum at rather small values of K [figure 3(d)-(e)]. By changing the neighborhood from block over adjacent to random, this maximum becomes more pronounced and is shifted slightly to larger K .

Concerning the different walk types, the behavior of $\langle h \rangle$ looks qualitatively similar at first glance. However, when comparing the walk types on the same landscape model a more interesting picture emerges. In the block model greedy walks attain a larger height than random AW's and reluctant walks reach the lowest heights, as would be expected from the results on the HoC landscape. For adjacent neighborhoods, the order of the heights remains the same, but the differences become smaller. However, for random neighborhoods, one can find values of K where this order is reversed, implying that the reluctant walks are most efficient in locating high fitness values (see figure 4). This effect was also observed previously for similar landscape models in a different context [57, 58].

3.3. Clustering of local maxima

In addition to the number of local fitness maxima, also their distribution in sequence space should be expected to affect the behavior of adaptive walks. Even on the uncorrelated HoC landscape, the probability that a randomly chosen genotype is a local maximum is given by $p_{\text{max}} = 1/(L + 1)$ while the probability that two genotypes at distance 2 are both maxima is given by $p_{\text{max},2} = 1/[L(L + 1)] > p_{\text{max}}^2$ [64], i.e., in the

proximity of a local maximum it is more probable to find another. This effect is weak on the HoC landscape, but on a correlated landscape the clustering of maxima can become quite pronounced, as has been repeatedly noted in the NK literature [19, 65].

For the block model, this effect is easy to quantify. A genotype σ is a fitness maximum, if and only if its blocks correspond to maxima in their sub-landscape. Hence the corresponding probability p_{\max} is given by

$$p_{\max} = \left(\frac{1}{K+1} \right)^{\frac{L}{K}}.$$

Now let τ be a second genotype that is randomly chosen under the constraint $d(\sigma, \tau) = 2$. In order to be a local maximum as well, the loci in which τ differs from σ have to be within the same block, which is fulfilled with probability $(K-1)/(L-1)$, and there must be another local maximum at this position in the block, which is true with probability $1/K$. Therefore, the probability $p_{\max,2}$ is given by

$$p_{\max,2} = p_{\max} \frac{K-1}{K(L-1)} \quad (13)$$

which is vastly larger than p_{\max}^2 for sufficiently large L . The clustering of local maxima can also be observed for the other neighborhood types. In figure 5(a) we display the distribution of distances between local maxima, showing that the clustering of maxima is strongest for the block neighborhood while it is weakest for the random neighborhood.

The analysis in figure 5(a) was restricted to rather small landscapes of size $L = 20$ where it is feasible to exhaustively sample all genotypes. For much larger landscapes this is no longer possible and it is very difficult to devise an unbiased search algorithm that randomly samples local maxima. For this reason, we simply consider local maxima that were found by an adaptive walk and determine the mean number N_{sur} of maxima surrounding such a maximum, i.e., those at the minimal distance $d = 2$. The result is shown in figure 5(b). Apparently, the walk type does not have a large impact on N_{sur} , but the neighborhood type does. For intermediate values of K , the number of surrounding maxima in the random neighborhood differs from the results for block neighborhoods by a factor of almost 50, while the results for the adjacent neighborhood lie, as always, roughly halfway between block and random neighborhood. To assess how strongly these results are biased by the sampling of the maxima by an AW, one may compare the numerical results for the block model to the corresponding prediction for randomly chosen local maxima derived from (13). It is seen in figure 5(b) that N_{sur} is slightly larger for randomly chosen maxima, implying that the maxima found during an AW are more isolated than the typical ones. Nevertheless, the effect of sampling bias appears to be rather minor, and we conclude that the study of N_{sur} exposes one of the most recognizable differences between neighborhood types.

3.4. Neighborhood rank

The rank r of NK-neighborhoods was introduced in [37] to quantify neighborhood schemes, and it was shown numerically to be negatively correlated to the number of

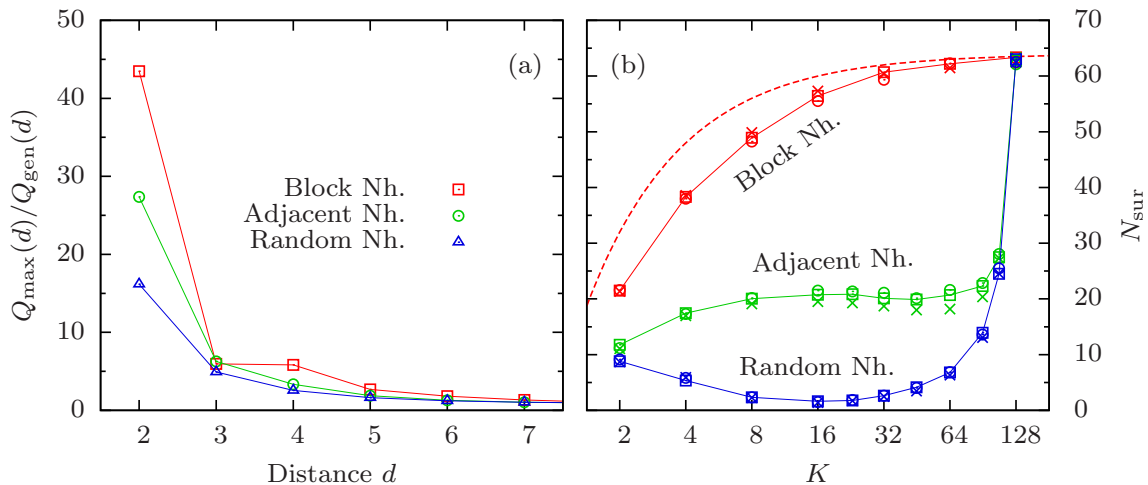


Figure 5. Clustering of local maxima. (a) Distribution Q_{\max} of the distance d between pairs of local maxima, normalized to the corresponding distribution Q_{gen} of all genotypes. Landscape parameters are $L = 20$ and $K = 5$. (b) Mean number N_{sur} of local maxima that are at distance $d = 2$ to the final genotype of an adaptive walk on an $L = 128$ landscape. Circles correspond to greedy, squares to random and crosses to reluctant walks, though the walk type does not have a large impact on the result. Solid lines are for visual guidance. The dashed line shows N_{sur} according to (13) for a randomly chosen maximum in the block model.

maxima of a landscape if K and L are kept constant. The rank of an NK neighborhood scheme is defined as

$$r(\mathbf{V}) = \left| \bigcup_{i=1}^L \mathcal{P}(V_i) \right|, \quad (14)$$

where $\mathcal{P}(M)$ and $|M|$ denote the power set and counting measure, respectively, of a set M . A more convenient but equivalent definition of the rank can be given in terms of the Fourier expansion (7), where it is equal to the number of non-zero coupling constants (including the H_i and F_0). In this section, we will first calculate the rank for the classic neighborhoods of block, adjacent and random type. We will then generate neighborhoods of arbitrary rank that interpolate between these types and show that the AW-based landscape measures considered in the previous sections are correlated to the rank as well.

3.4.1. Calculation of the rank

Block neighborhood: For the block model the rank is straightforward to obtain. Each block contains every subset of size smaller or equal to K , giving a contribution of 2^K to the rank. Since there are L/K blocks and the empty set is counted only once, we obtain

$$r_{\text{blc}} = \frac{L}{K} (2^K - 1) + 1. \quad (15)$$

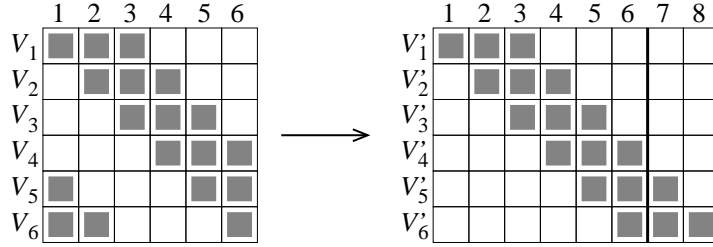


Figure 6. Illustration of the calculation of the rank for the adjacent neighborhood model. A grey square in the i -th row and j -th column means that V_i and V'_i , respectively, contains j . The left panel shows an adjacent neighborhood scheme for $L = 6$ and $K = 3$, and the right panel shows the extended scheme for which the rank is actually calculated.

Adjacent neighborhood: We will show that the rank of the adjacent neighborhood is given by

$$r_{\text{adj}} = 1 + L \cdot 2^{K-1} \quad (16)$$

for $K \leq (L + 1)/2$. For the calculation we define sets V'_i which are the same as the standard neighborhood sets V_i from (5) but without taking the elements modulo L , i.e., the V'_i contain elements up to $L + K - 1$ (see figure 6). Furthermore define

$$\mathcal{M}' = \left\{ M \in \bigcup_{i=1}^N \mathcal{P}(V'_i) \mid \min(M) \leq L \right\}. \quad (17)$$

It is straightforward to count the number of elements in \mathcal{M}' . A set $M \subset \mathbb{N}$ is contained in \mathcal{M}' if and only if

$$1 \leq \min(M) \leq L \quad \text{and} \quad \max(M) - \min(M) < K. \quad (18)$$

For given $a = \min(M)$ and $b = \max(M)$, there are 2^{b-a-1} possible sets. Summing over all a and b which fulfill (18) leads to

$$\begin{aligned} |\mathcal{M}'| &= 1 + L + \sum_{a=1}^L \sum_{b=a+1}^{a+K-1} 2^{b-a-1} \\ &= 1 + L + L \cdot \sum_{d=0}^{K-2} 2^d = 1 + L \cdot 2^{K-1}. \end{aligned} \quad (19)$$

We will now show that indeed $|\mathcal{M}'| = |\mathcal{M}| = r_{\text{adj}}$ for $K \leq (L + 1)/2$. Note, however, that $|\mathcal{M}'| > |\mathcal{M}|$ for $K > (L + 1)/2$ and hence (19) overestimates the actual rank in this case. We define the function $\text{mod}: \mathcal{M}' \rightarrow \mathcal{M}$ by

$$\text{mod}(M') = \{i \bmod L \mid i \in M'\} \quad (20)$$

and show that it is bijective if $K \leq (L + 1)/2$. In fact the mod-function is always surjective, but only injective if $K \leq (L + 1)/2$. Let $M = \{m_1, \dots, m_n\} \in \mathcal{M}$ with $m_1 < m_2 < \dots < m_n$. Define

$$M' = \begin{cases} M & m_n - m_1 < K \\ \{g(m_1), \dots, g(m_n)\} & \text{else} \end{cases} \quad (21)$$

where

$$g(m) = \begin{cases} m & \text{if } m \geq K \\ m + L & \text{else.} \end{cases} \quad (22)$$

Since $M' \in \mathcal{M}'$ and $\text{mod}(M') = M$, the function is surjective and hence $|\mathcal{M}'| \geq |\mathcal{M}|$. Now let $A = \{a_1, \dots, a_n\}$ and $B = \{b_1, \dots, b_n\}$, where $a_k < a_{k+1}$ and $b_k < b_{k+1}$ for all k , be two elements of \mathcal{M}' with $\text{mod}(A) = \text{mod}(B)$. We will show that either $A = B$ or $K > (L + 1)/2$, i.e., mod is injective if $K \leq (L + 1)/2$. We denote by i and j the smallest indices that fulfill $a_i \geq L$ and $b_j \geq L$, respectively, which means that

$$\begin{aligned} \text{mod}(A) &= \{a_i - L, \dots, a_n - L, a_1, \dots, a_{i-1}\} \\ &= \{b_j - L, \dots, b_n - L, b_1, \dots, b_{j-1}\} = \text{mod}(B). \end{aligned} \quad (23)$$

Note that the elements of $\text{mod}(A)$ and $\text{mod}(B)$ are written in ascending order in (23). Therefore, it is obvious that $A = B$ if $i = j$ and thus we assume without loss of generality that $i < j$. By comparison of the elements one finds that $a_n - L = b_{j-i}$ and $a_1 = b_{j-i+1}$. Because both A and B are elements of \mathcal{M}' , the conditions $a_n - a_1 = b_{j-i} - b_{j-i+1} + L < K$ and $b_{j-i+1} - b_{j-i} < K$ have to be fulfilled which finally leads to

$$K > b_{j-i+1} - b_{j-i} > L - K \quad \Rightarrow \quad K > \frac{L + 1}{2}. \quad (24)$$

Random neighborhood: Due to the random choice of neighbors, the rank is a random variable in this case, and we will calculate its expectation value. First the probability that a given set W is a subset of V_i is needed. Since V_i always contains i , the probability depends on whether $i \in W$ or not. We find

$$\mathbb{P}(W \subset V_i \mid i \in W) = \frac{(K - 1)! (L - m)!}{(L - 1)! (K - m)!} =: p_m \quad (25)$$

and

$$\mathbb{P}(W \subset V_i \mid i \notin W) = \frac{(K - 1)! (L - 1 - m)!}{(L - 1)! (K - 1 - m)!} = p_m \cdot \frac{K - m}{L - m}, \quad (26)$$

where m is the number of elements of W . Hence the probability q_m that W is contained in at least one of the neighborhood sets is given by

$$\begin{aligned} q_m &= \mathbb{P}(\exists i: W \subset V_i) \\ &= \mathbb{P}(\exists i \in W: W \subset V_i) + \mathbb{P}(\exists i \notin W: W \subset V_i) \\ &= 1 - (1 - p_m)^m + \left[1 - \left(1 - p_m \cdot \frac{K - m}{L - m} \right)^{L - m} \right] \end{aligned} \quad (27)$$

for $m \geq 2$ and obviously $q_0 = q_1 = 1$. There are $\binom{L}{m}$ such subsets W for each size m and hence the mean rank is given by

$$r_{\text{rnd}} = \sum_{m=0}^K \binom{L}{m} q_m = 1 + L + \sum_{m=2}^K \binom{L}{m} q_m. \quad (28)$$

The result can be simplified by using the approximation $(1-x)^n \approx 1-nx$ in (27), which is valid when p_m is very small. This yields $q_m \approx K \cdot p_m$ and hence

$$r_{\text{rnd}} \approx 1 + L + \sum_{m=2}^K \binom{L}{m} \frac{K!}{(L-1)!} \frac{(L-m)!}{(K-m)!} \quad (29)$$

$$= 1 + L (2^K - K) = r_{\text{max}}, \quad (30)$$

where r_{max} is the upper limit for the rank of a neighborhood with fixed L and K [37].

3.4.2. Correlation between walk properties and rank. Literally all quantities we analyzed in section 3.2 were either minimal or maximal for block and random neighborhoods, with the values for the adjacent model lying in between. It is therefore not surprising that the same holds true for the rank, which is minimal for block and maximal for random neighborhoods. This is not a coincidence, as most quantities seem to be generally correlated to the rank, as we are now going to show by analyzing neighborhoods with arbitrary rank. To generate these neighborhoods, we use the following algorithm:

- (i) Start with a block neighborhood.
- (ii) Choose randomly a set V_i , an element $n \in V_i$ with $n \neq i$, and replace it by another element $m \notin V_i$.
- (iii) If the rank has been increased due to this operation, the change in V_i is accepted. Otherwise, the change is undone.
- (iv) If no rank increasing changes are found in 1000 successive trials, we start again at step (i). Otherwise, we continue with step (v).
- (v) When the rank hits a prescribed threshold, an adaptive walk is performed with the current neighborhood sets.
- (vi) Go to step (ii).

With this method, we can produce thousands of different neighborhood schemes with ranks between r_{blc} and r_{max} , although the maximal rank that can be achieved in this way is usually somewhat below r_{max} . The results are shown in figure 7. Clearly, all quantities considered in section 3.2, i.e., the mean walk length $\langle \ell \rangle$, height $\langle h \rangle$ and the number N_{sur} of local maxima at distance $d = 2$ to the final genotype of the walk, are strongly related to the rank and either increase or decrease monotonically with r . For both height and length it turns out that the different walk types react differently to variations of the rank, whereas N_{sur} , similar to the results shown in figure 5(b), is largely independent of the walk type. The length of greedy and random adaptive walks increases roughly linearly with rank, with a larger slope for random AW's. Reluctant walks are more susceptible to alterations of the rank, the dependence of walk length on r being stronger than linear.

Walk heights show a similar behavior as the length in terms of the sensitivity of different walk types. Reluctant walks do show a roughly linear dependence on the rank

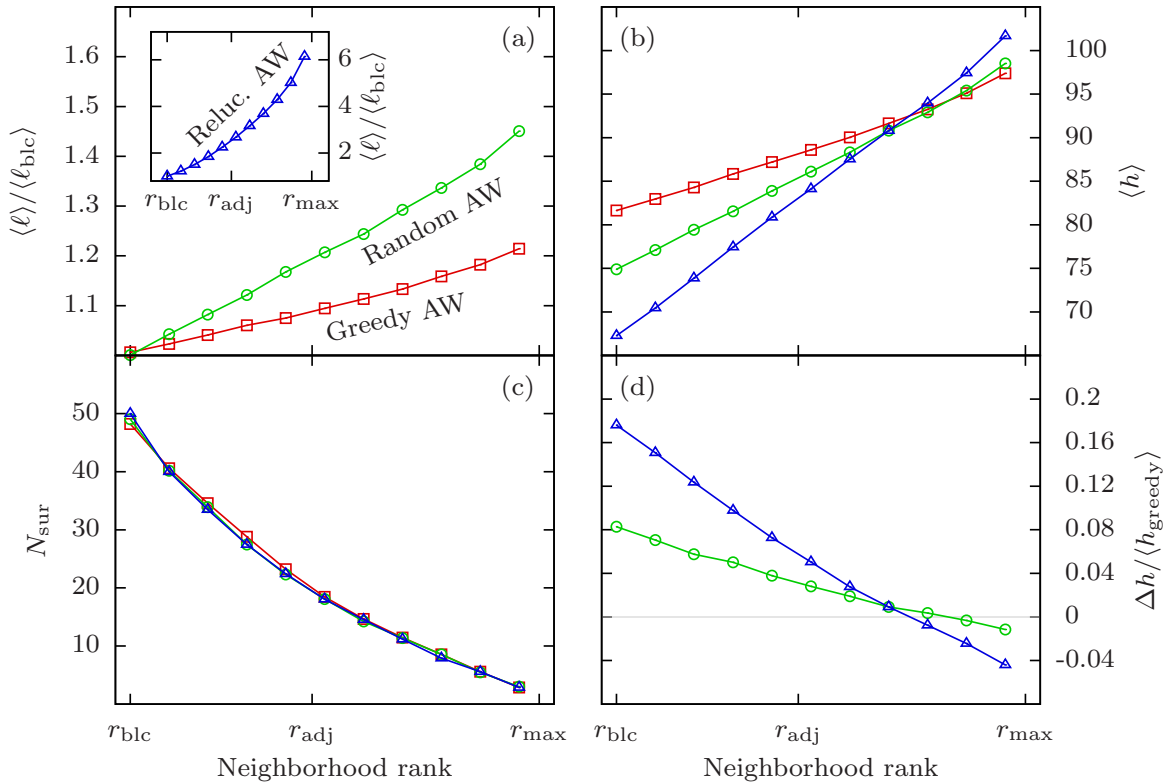


Figure 7. Correlation between the rank and several properties of adaptive walks on an $L = 128$, $K = 8$ landscape. The quantities shown are (a) the mean walk length $\langle \ell \rangle$, (b) the mean walk height $\langle h \rangle$, (c) the number N_{sur} of maxima at distance $d = 2$ to the final genotype of the walk and (d) the height advantage Δh of greedy adaptive walks. Lines are for visual guidance.

here, but the slope is larger than that for random and greedy walks. Since reluctant and random walks reach a lower height for the minimal rank r_{blc} , their height-rank curve may have a point of intersection with the curve for the greedy walk. This point marks the threshold where reluctant and random AW's become more successful in their ability to find large fitness values. Such a point exists for the landscape parameters $L = 128$ and $K = 8$ chosen here, but not in general. As suggested by figure 4, an intermediate value of K compared to L is needed to observe this phenomenon, and L has to be sufficiently large.

4. Summary and discussion

In this paper we studied different adaptive walk models on the NK landscape with the focus on the differences between interaction schemes of the NK model. In section 3.2 we analyzed three classic neighborhood types as well as three walk types, resulting in nine different combinations. The picture that we obtain is nevertheless rather simple: For each walk type, both the mean walk length $\langle \ell \rangle$ and height $\langle h \rangle$ are largest for random,

second largest for adjacent and smallest for block neighborhoods, while the order is reversed for the number N_{sur} of maxima surrounding the final genotype of a walk. Similarly, for each neighborhood type, $\langle \ell \rangle$ is largest for reluctant, second largest for random and smallest for greedy walks. In most situations, the opposite ordering applies to $\langle h \rangle$, but for random neighborhoods and certain values of K and L this order can be reversed and reluctant walks become the most successful ones in terms of height.

In section 3.4 we showed that this picture can be extended to more general choices of the neighborhood which can be classified in terms of the rank. Block, adjacent and random neighborhoods are just examples of schemes with low, medium and high rank, respectively. Our findings concerning the relation between walk length and rank are consistent with results from previous work, since ℓ would be expected to be related to the density of local maxima which decreases slightly with increasing rank [37]. In this sense, an increasing rank decreases the ruggedness of a landscape. Note that this is also consistent with another measure of ruggedness, namely the probability to find an accessible path to the global maximum, which was found to be largest for random, second largest for adjacent and smallest for block neighborhoods [36].

If the number of local maxima decreases with increasing rank, one would expect the same trend for the number of maxima N_{sur} surrounding a given maximum. Though this is true, the effect on N_{sur} is much stronger than that on the walk length and the number of maxima, which indicates that the rank affects the distribution of maxima in the landscape more substantially than their density. Maxima become much more isolated with increasing rank. The fact that N_{sur} hardly depends on the walk type suggests that this is true for typical local maxima and not only for those found by adaptive walks.

The rank thus appears to be a powerful tool for the characterization and description of neighborhood schemes, but so far it lacks explanatory power. In fact, it is quite surprising that the ruggedness decreases with the rank for fixed L and K , since the opposite is true if the neighborhood type is fixed and the rank is increased due to an increase of K [66]. Because of the difficulty of analytical approaches to the NK model for neighborhoods that are not block-like as well as the impossibility to exhaustively enumerate the entire landscape for large L , we are for now restricted to indirect measurements using adaptive walks. Nevertheless, we showed that the model is rich in interesting and non-trivial phenomena and hope that the dependence of landscape properties on interaction schemes will be investigated more frequently in future work.

With regard to the application of probabilistic models for the interpretation of empirical fitness landscapes, our work highlights the importance of developing refined measures of genetic interactions that go beyond the summary statistics of fitness landscape ruggedness considered in most previous studies [2, 3]. Moreover, our demonstration that different types of adaptive walks respond differently to the structure of these interactions suggests a new methodology for exploring high-dimensional empirical data sets, where adaptive walks have so far been employed only for estimating the correlation length and overall density of local maxima in the landscape [67].

Acknowledgments

We thank Cristian Giardina for pointing us to the literature on reluctant adaptive walks. This work was supported by DFG within SPP 1590 *Probabilistic structures in evolution*.

Appendix A. Adaptive walks on the HoC landscape

Here we derive several quantities for adaptive walks on the uncorrelated House-of-Cards landscape. Although the properties of the walks do not depend on the underlying fitness distribution, for convenience the fitness values are assumed to be uniformly distributed on the interval $[0, 1]$.

Appendix A.1. Height of greedy adaptive walks

To calculate the mean walk height for greedy adaptive walks is rather simple. If the walk has a length ℓ , the population sees in total $(\ell + 1) \cdot L$ genotypes and chooses the one with largest fitness. The mean value of the largest of n i.i.d. uniform random variables is given by $M_n = n/(n + 1)$, the probability that the walk has length ℓ is given by $P_\ell = \ell/(\ell + 1)!$ [62] and hence the mean walk height is given by

$$\langle h \rangle = \sum_{\ell=0}^{\infty} M_{(\ell+1) \cdot L} \cdot P_\ell = 1 - \sum_{\ell=0}^{\infty} \frac{1}{(\ell + 1) \cdot L + 1} \cdot \frac{\ell}{(\ell + 1)!} \quad (\text{A.1})$$

$$\approx 1 - \sum_{\ell=0}^{\infty} \frac{1}{(\ell + 1) \cdot L} \cdot \frac{\ell}{(\ell + 1)!} = 1 - \frac{\alpha_{\text{grd}}}{L} \quad (\text{A.2})$$

where

$$\alpha_{\text{grd}} = \sum_{\ell=0}^{\infty} \frac{\ell}{(\ell + 1) \cdot (\ell + 1)!} = 0.4003 \dots \quad (\text{A.3})$$

Appendix A.2. Height of random adaptive walks

The probability density $q_N(x)$ for the height of random adaptive walks on a uniformly distributed HoC landscape is known [61], so we will just compute its average. The density function of the height is given by

$$q_L(x) = x^{L-1} \cdot \exp\left(\sum_{k=1}^{L-1} \frac{x^k}{k}\right). \quad (\text{A.4})$$

In order to compute the mean value, we define

$$r_L(x) := \frac{q_L(1 - x/L)}{q_L(1)} = \left(1 - \frac{x}{L}\right)^{L-1} \exp\left(\sum_{k=1}^{L-1} \frac{\left(1 - \frac{x}{L}\right)^k - 1}{k}\right). \quad (\text{A.5})$$

The exponent can be written as

$$\xi(x, L) := \sum_{k=1}^{L-1} \frac{\left(1 - \frac{x}{L}\right)^k - 1}{k} \quad (\text{A.6})$$

$$= \sum_{k=1}^{L-1} \sum_{s=1}^k \frac{(k-1)!}{s! \cdot (k-s)!} (-1)^s \left(\frac{x}{L}\right)^s \quad (\text{A.7})$$

$$= \sum_{s=1}^{L-1} \sum_{k=s}^{L-1} \frac{(k-1)!}{s! \cdot (k-s)!} (-1)^s \left(\frac{x}{L}\right)^s \quad (\text{A.8})$$

$$= \sum_{s=1}^{L-1} \frac{(-1)^s x^s}{s \cdot s!} \cdot \frac{(L-1)!}{L^s (L-s-1)!} \quad (\text{A.9})$$

The second factor is smaller than 1 and bounded from below by $1 - s^2/L$, i.e.,

$$\sum_{s=1}^{L-1} \frac{(-1)^s x^s}{s \cdot s!} \geq \xi(x, L) \geq \left(\sum_{s=1}^{L-1} \frac{(-1)^s x^s}{s \cdot s!} \right) - R(x, L) \quad (\text{A.10})$$

with the remainder term

$$R(x, L) = -\frac{1}{L} \sum_{s=1}^{L-1} \frac{(-1)^s x^s}{(s-1)!}. \quad (\text{A.11})$$

Since

$$\lim_{L \rightarrow \infty} LR(x, L) = -\sum_{s=1}^{\infty} \frac{(-1)^s x^s}{(s-1)!} = x e^{-x} \quad (\text{A.12})$$

is finite, $R(x, L)$ tends to zero for $L \rightarrow \infty$. By the squeeze theorem it follows that

$$\lim_{L \rightarrow \infty} \xi(x, L) = \sum_{s=1}^{\infty} \frac{(-1)^s x^s}{s \cdot s!} = -(\log(x) + \Gamma(0, x) + \gamma) \quad (\text{A.13})$$

where $\gamma \approx 0.5772\dots$ is the Euler-Mascheroni constant and $\Gamma(a, z) = \int_z^{\infty} t^{a-1} e^{-t} dt$ is the incomplete gamma function. Hence the function series r_L converges for $L \rightarrow \infty$ to a non-degenerate limiting function

$$r_{\infty}(x) = \exp(-x - \log(x) - \Gamma(0, x) - \gamma). \quad (\text{A.14})$$

Since r_{∞} does not depend on L , we can extract the L -dependence of q . With the substitution $x = 1 - y/L$ we find

$$\langle h \rangle = \int_0^1 x q_L(x) dx = \frac{1}{L} \int_0^L \left(1 - \frac{y}{L}\right) \cdot q_L\left(1 - \frac{y}{L}\right) dy \quad (\text{A.15})$$

$$= 1 - \frac{q_L(1)}{L^2} \int_0^L y r_L(y) dy \approx 1 - \frac{e^{\gamma}}{L} \int_0^{\infty} y r_{\infty}(y) dy \quad (\text{A.16})$$

$$= 1 - \frac{\alpha_{\text{rnd}}}{L} \quad (\text{A.17})$$

with

$$\alpha_{\text{rnd}} = \int_0^{\infty} \exp(-x - \Gamma(0, x)) dx = 0.6243\dots \quad (\text{A.18})$$

This result was previously obtained in [60].

Appendix A.3. Reluctant walks

For the reluctant walk on the HoC landscape, we find numerically that the length is asymptotically given by $\langle \ell \rangle = L/2$ and the height by $\langle h \rangle = 1 - 1/L$ (see figure A1). These results are plausible within the Gillespie approximation [7, 8], a simplified setting where the entire adaptive walk proceeds among a single set of L random fitness values; in other words, the creation of a new neighborhood of independently drawn fitness values after each step is neglected. Somewhat surprisingly, the Gillespie approximation has been shown to correctly reproduce the leading order $\log L$ -behavior for the length of random and natural AW's [8, 52]. For the greedy AW it trivially predicts $\ell = 1$, which is also rather close to the exact result $\langle \ell \rangle = e - 1 \approx 1.7183$. Within the Gillespie approximation, a reluctant walk visits all sites of the neighborhood in order of increasing fitness, and the walk length is equal to the rank of the initial fitness among the other L fitness values in the neighborhood minus one. It follows that the length is $L/2$ on average.

As a starting point for a systematic treatment of reluctant AW's on the HoC landscape, we derive a recurrence relation for the quantity

$$P_\ell(x) := \mathbb{P}(\text{fitness in } [x, x + dx] \text{ after } \ell \text{ steps}), \quad (\text{A.19})$$

following the procedure of Flyvbjerg and Lautrup [61]. The recurrence relation in general reads

$$P_{\ell+1}(x) = \int_{-\infty}^x P_\ell(y) \gamma(y \rightarrow x) dy \quad (\text{A.20})$$

where $\gamma(y \rightarrow x)$ is the probability density of the smallest of N random variables that is larger than y . For uniform random variables and conditioned on there being $k > 0$ random variables larger than y , the density is given by

$$\gamma(y \rightarrow x | k) = \frac{k}{1-y} \left(1 - \frac{x-y}{1-y}\right)^{k-1} \quad (\text{A.21})$$

and hence

$$\gamma(y \rightarrow x) = \sum_{k=1}^N \binom{N}{k} (1-y)^k y^{N-k} \gamma(y \rightarrow x | k) \quad (\text{A.22})$$

$$= \sum_{k=1}^N \binom{N}{k} k (1-x)^{k-1} y^{N-k} \quad (\text{A.23})$$

$$= N (1-x+y)^{N-1}. \quad (\text{A.24})$$

Then equation (A.20) becomes

$$P_{\ell+1}(x) = N \int_0^x P_\ell(y) (1-x+y)^{N-1} dy \quad (\text{A.25})$$

from which quantities of interest like walk lengths and heights could in principle be extracted. However, so far we have not succeeded in solving the recursion (A.25).

Appendix A.4. Walk height for fitness distributions in the Gumbel class

So far, the calculations of the mean value of the walk height h were based on the assumption that the fitness values are uniformly distributed. Obviously, fitness values drawn from another continuous distribution can always be transformed to the uniform case (and vice versa), since for a random variable X with cumulative distribution function Q the distribution of $Q(X)$ is uniform. Therefore, the transformed height $Q(h)$ for an arbitrary distribution has the same probability density function $q(x)$ as the height in the uniform case. One could in principle get to the mean height h by

$$\langle h \rangle = \langle Q^{-1}(Q(h)) \rangle = \int_0^1 Q^{-1}(x) q(x) dx, \quad (\text{A.26})$$

but in practice this integral can be cumbersome to evaluate. However, for fitness values drawn from a distribution in the Gumbel class of extreme value theory, e.g., a Gaussian distribution, there is a simple approximation for the relation between h and $Q(h)$.

Let X_1, \dots, X_n be i.i.d. random variables with cumulative distribution function $Q = 1 - \exp(-\lambda x)$ and $M_n = \max(X_1, \dots, X_n)$. The mean value of $Q(M_n)$ is given by

$$\langle Q(M_n) \rangle = 1 - \frac{1}{n+1} \quad (\text{A.27})$$

whereas the mean value of M_n is given by [63]

$$\lambda \langle M_n \rangle = H_n = \sum_{k=1}^n \frac{1}{k} = \log n + \gamma + \mathcal{O}\left(\frac{1}{n}\right) \quad (\text{A.28})$$

where H_n is the n -th harmonic number. This yields

$$Q(\langle M_n \rangle) \approx 1 - \frac{e^{-\gamma}}{n} \approx 1 - e^{-\gamma} (1 - \langle Q(M_n) \rangle). \quad (\text{A.29})$$

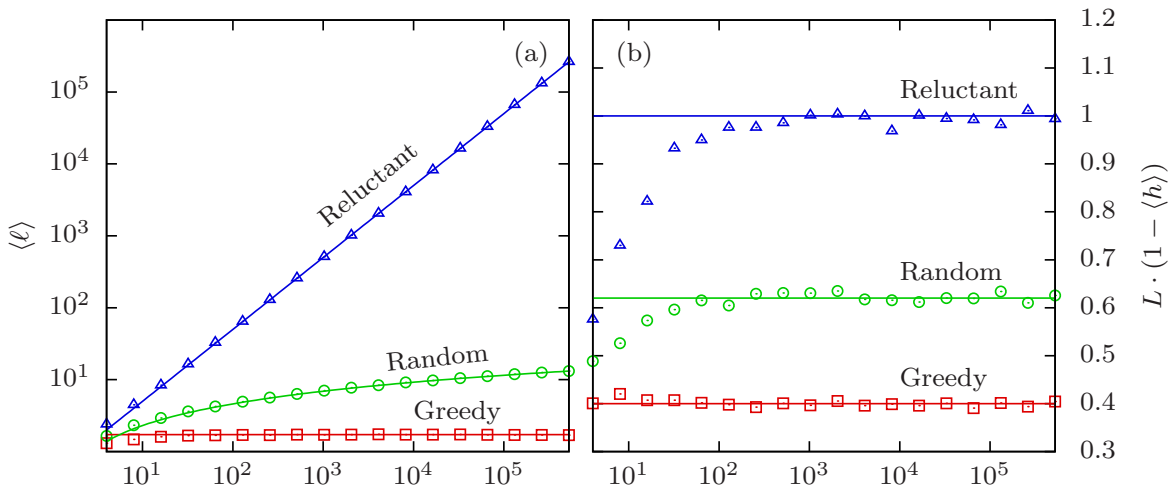


Figure A1. (a) Mean walk length $\langle \ell \rangle$ and (b) height $\langle h \rangle$ on the House-of-Cards landscape. The numerical results suggest that $\langle \ell \rangle = \frac{L}{2}$ and $\langle h \rangle = 1 - \frac{1}{L}$ for the reluctant walk.

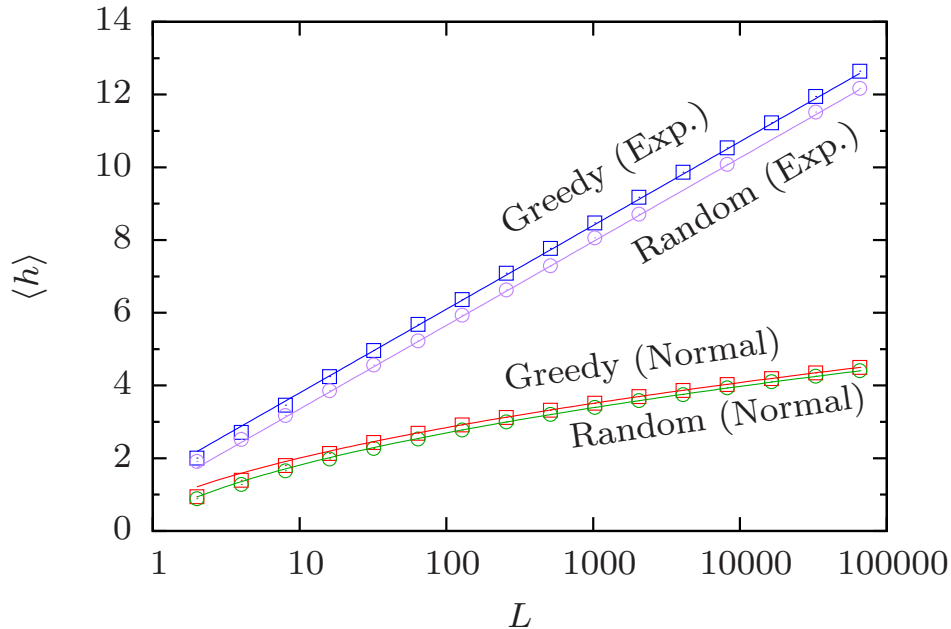


Figure A2. Height of random and greedy adaptive walks on the HoC landscape with fitness values distributed according to a standard normal distribution and a standard exponential distribution, respectively. Symbols correspond to simulation results, lines correspond to (A.30).

Because the Pickands-Balkema-de Haan theorem [63, 68, 69] states that the tail of a distribution from the Gumbel class is well described by the exponential distribution, this approximation is also valid for more general choices of Q if n is large. We now assume that h behaves statistically like the maximum of n random variables, i.e., like M_n . Although n is not necessarily known in the case of adaptive walks, we can still use (A.29) to obtain

$$\langle h \rangle \approx Q^{-1} \left[1 - e^{-\gamma} (1 - \langle Q(h) \rangle) \right] = Q^{-1} \left[1 - \frac{\alpha e^{-\gamma}}{L} \right], \quad (\text{A.30})$$

where α is the factor depending on the walk type that was derived above. Despite the somewhat uncontrolled nature of the approximation, the result is quite precise as shown in figure A2.

Appendix B. Number of maxima in the adjacent NK-model with $K = 2$

In the adjacent NK model with $K = 2$, the fitness $F(\sigma)$ of a genotype $\sigma \in \mathbb{H}_L$ is given by

$$F(\sigma) = \sum_{i=1}^L \eta_i(\sigma_i, \sigma_{i+1}), \quad (\text{B.1})$$

where $\sigma_{L+1} = \sigma_1$ and the $\eta_i(\sigma, \tau)$ are random numbers independently drawn from a distribution with density function f for each i , σ and τ , i.e., one needs $4L$ random

numbers to specify the whole model. In the following we will show that, if the random numbers are drawn from a Gamma distribution with shape parameter $p = 1/2$, the mean number N_{\max} of local maxima in such a landscape is given by

$$N_{\max} = (2\lambda_+)^L + (2\lambda_-)^L, \quad (\text{B.2})$$

where

$$\lambda_{\pm} = \frac{1}{6} \left[3 - \sqrt{3} \pm \sqrt{6(\sqrt{3} - 1)} \right]. \quad (\text{B.3})$$

In order to derive this result, we consider a specific genotype σ which without loss of generality can be chosen as the all-zero genotype $\sigma = (0, \dots, 0)$, and calculate the probability P_{\max} that it is a local optimum. Its fitness is determined by the sum of L random numbers, which will be denoted by $x_i = \eta_i(0, 0)$ and is fixed in the following. If a mutation occurs at position j of the genome, the contributions x_{j-1} and x_j (with $x_0 = x_L$) are replaced by two new random variables x'_{j-1} and x'_j , respectively. Obviously, if σ is a local optimum, $x'_{j-1} + x'_j < x_{j-1} + x_j$ must hold true. Since the x_i are fixed, this probability can be written as

$$\mathbb{P}(x'_{j-1} + x'_j < x_{j-1} + x_j) = \tilde{F}(x_{j-1} + x_j), \quad (\text{B.4})$$

where

$$\tilde{F}(x) = \int_{-\infty}^x \left(\int_{-\infty}^{\infty} f(z) f(y-z) dz \right) dy \quad (\text{B.5})$$

is the cumulative distribution function of the convolution of two random variables drawn from f . Note that the x'_i which can occur due to mutations are independent and therefore the probability that σ is a maximum [for fixed $\underline{x} = (x_1, \dots, x_L)$] is given by

$$P_{\max}(\underline{x}) = \tilde{F}(x_1 + x_2) \tilde{F}(x_2 + x_3) \cdots \tilde{F}(x_{L-1} + x_L) \tilde{F}(x_L + x_1). \quad (\text{B.6})$$

The actual probability P_{\max} can then be obtained by integrating over all values of \underline{x} , i.e.,

$$P_{\max} = \int_{\mathbb{R}^L} \prod_{n=1}^L \left(f(x_n) \tilde{F}(x_n + x_{n+1}) \right) d^L \underline{x}. \quad (\text{B.7})$$

This integral can be solved exactly if the contributions are drawn from a Gamma distribution with shape parameter $p = 1/2$, i.e., the density function f is given by

$$f(x) = \frac{\exp(-x)}{\sqrt{\pi x}} \quad (\text{B.8})$$

for $x > 0$ and zero otherwise. The sum of two random variables drawn from this distribution is exponentially distributed, i.e.,

$$\tilde{F}(x) = 1 - e^{-x} \quad (\text{B.9})$$

and equation (B.7) becomes

$$P_{\max} = \frac{1}{\sqrt{\pi^L}} \int_{\mathbb{R}_+^L} \prod_{n=1}^L \left(\frac{\exp(-x_n)}{\sqrt{x_n}} (1 - e^{-x_n - x_{n+1}}) \right) d^L \underline{x}. \quad (\text{B.10})$$

Expanding the product yields

$$\prod_{n=1}^L (1 - e^{-x_n - x_{n+1}}) = \sum_{\sigma} \prod_{n=1}^L (-1)^{\sigma_n} e^{-x_n(\sigma_{n-1} + \sigma_n)}, \quad (\text{B.11})$$

where the sum goes over all $\sigma \in \{0, 1\}^L$. Inserting (B.11) into (B.10) gives

$$P_{\max} = \frac{1}{\sqrt{\pi^L}} \int_{\mathbb{R}_+^L} \sum_{\sigma} \prod_{n=1}^L \frac{(-1)^{\sigma_n}}{\sqrt{x_n}} e^{-x_n(\sigma_{n-1} + \sigma_n + 1)} d^L \underline{x} \quad (\text{B.12})$$

$$= \frac{1}{\sqrt{\pi^L}} \sum_{\sigma} \prod_{n=1}^L (-1)^{\sigma_n} \int_0^{\infty} \frac{\exp(-x(\sigma_{n-1} + \sigma_n + 1))}{\sqrt{x}} dx \quad (\text{B.13})$$

$$= \sum_{\sigma} \prod_{n=1}^L \frac{(-1)^{\sigma_n}}{\sqrt{\sigma_{n-1} + \sigma_n + 1}} = \sum_{\sigma} \prod_{n=1}^L T_{\sigma_n, \sigma_{n+1}} \quad (\text{B.14})$$

with the matrix

$$T = \begin{pmatrix} 1 & -\frac{1}{\sqrt{2}} \\ \frac{1}{\sqrt{2}} & -\frac{1}{\sqrt{3}} \end{pmatrix}. \quad (\text{B.15})$$

Equation (B.14) is of the form of a partition function of a spin chain and T is the corresponding transfer matrix. Using this analogue, one can write

$$P_{\max} = \text{Tr}(T^L) = \lambda_+^L + \lambda_-^L \quad (\text{B.16})$$

where λ_{\pm} are the eigenvalues of T which are given by equation (B.3). The final result is obtained by multiplying the probability P_{\max} with the total number 2^L of genotypes which yields

$$N_{\max} = P_{\max} \cdot 2^L = (2\lambda_+)^L + (2\lambda_-)^L. \quad (\text{B.17})$$

For large L the behavior is governed by the larger eigenvalue $\lambda_+ = 0.5606 \dots$

References

- [1] Wright S 1932 The roles of mutation, inbreeding, crossbreeding, and selection in evolution. *Proceedings of the Sixth International Congress on Genetics* vol 1 pp 355–366
- [2] Szendro I G, Schenk M F, Franke J, Krug J and de Visser J A G M 2013 *J. Stat. Mech.:Theory Exp.* P01005
- [3] de Visser J A G M and Krug J 2014 *Nature Reviews Genetics* **15** 480–490
- [4] Kimura M 1962 *Genetics* **47** 713
- [5] Sella G and Hirsh A E 2005 *Proceedings of the National Academy of Sciences of the United States of America* **102** 9541–9546
- [6] Wright S 1955 Classification of the factors of evolution. *Cold Spring Harbor Symposia on Quantitative Biology* vol 20 (Cold Spring Harbor Laboratory Press) pp 16–24
- [7] Gillespie J H 1983 *Theoretical Population Biology* **23** 202 – 215
- [8] Orr H A 2002 *Evolution* **56** 1317–1330
- [9] Weinreich D M, Delaney N F, DePristo M A and Hartl D L 2006 *Science* **312** 111–114
- [10] Poelwijk F J, Kiviet D J, Weinreich D M and Tans S J 2007 *Nature* **445** 383–386
- [11] Lozovsky E R, Chookajorn T, Brown K M, Imwong M, Shaw P J, Kamchonwongpaisan S, Neafsey D E, Weinreich D M and Hartl D L 2009 *Proceedings of the National Academy of Sciences* **106** 12025–12030

- [12] Carneiro M and Hartl D L 2010 *Proceedings of the National Academy of Sciences* **107** 1747–1751
- [13] Hall D W, Agan M and Pope S C 2010 *Journal of Heredity* **101** S75–S84
- [14] Chou H H, Chiu H C, Delaney N F, Segrè D and Marx C J 2011 *Science* **332** 1190–1192
- [15] Khan A I, Dinh D M, Schneider D, Lenski R E and Cooper T F 2011 *Science* **332** 1193–1196
- [16] Kingman J F C 1978 *Journal of Applied Probability* **15** 1–12
- [17] Kauffman S and Levin S 1987 *Journal of Theoretical Biology* **128** 11 – 45
- [18] Kauffman S A and Weinberger E D 1989 *Journal of Theoretical Biology* **141** 211 – 245
- [19] Kauffman S A 1993 *The Origins of Order* (New York: Oxford University Press)
- [20] Stein D L 1992 *Spin Glasses and Biology* (Singapore: World Scientific)
- [21] Derrida B 1981 *Phys. Rev. B* **24** 2613–2626
- [22] Stadler P F and Happel R 1999 *Journal of Mathematical Biology* **38** 435–478
- [23] Weinberger E D 1996 NP completeness of Kauffman’s NK model, a tuneable rugged fitness landscape. Santa Fe Institute Working Paper 96-02-003 URL <http://www.santafe.edu/media/workingpapers/96-02-003.pdf>
- [24] Altenberg L 1997 NK fitness landscapes. *Handbook of Evolutionary Computation* ed Bäck T, Fogel D B and Michalewicz Z (IOP Publishing Ltd and Oxford University Press)
- [25] Heckendorn R and Whitley D 1997 A Walsh analysis of NK landscapes. *Proceedings of the Seventh International Conference on Genetic algorithms* ed Bäck T (Morgan Kaufmann) pp 41–48
- [26] Wright A H, Thompson R K and Zhang J 2000 *IEEE Transactions on Evolutionary Computation* **4** 373–379
- [27] Perelson A S and Macken C A 1995 *Proceedings of the National Academy of Sciences* **92** 9657–9661
- [28] Evans S N and Steinsaltz D 2002 *The Annals of Applied Probability* **12** 1299–1321
- [29] Durrett R and Limic V 2003 *Ann. Probab.* **31** 1713–1753
- [30] Limic V and Pemantle R 2004 *Ann. Probab.* **32** 2149–2178
- [31] Welch J J and Waxman D 2005 *J. Theor. Biol.* **234** 329–340
- [32] Orr H A 2006 *Evolution* **60** 1113–1124
- [33] Kaul H and Jacobson S H 2006 *Mathematical Programming* **106** 319–338
- [34] Franke J and Krug J 2012 *Journal of Statistical Physics* **148** 706–723
- [35] Neidhart J, Szendro I G and Krug J 2013 *Journal of Theoretical Biology* **332** 218–227
- [36] Schmiegelt B and Krug J 2014 *Journal of Statistical Physics* **154** 334–355
- [37] Buzas J S and Dinitz J 2014 *IEEE Transactions on Evolutionary Computation* **18** 807–818
- [38] Fontana W, Stadler P, Bornberg-Bauer E, Griesmacher T, Hofacker I, Tacker M, Tarazona P, Weinberger E and Schuster P 1993 *Phys. Rev. E* **47** 2083–2099
- [39] Campos P R, Adami C and Wilke C O 2002 *Physica A: Statistical Mechanics and its Applications* **304** 495 – 506
- [40] Campos P R, Adami C and Wilke C O 2003 *Physica A: Statistical Mechanics and its Applications* **318** 637
- [41] Schoustra S E, Bataillon T, Gifford D R and Kassen R 2009 *PLoS Biol.* **7** e1000250
- [42] Franke J, Klözer A, de Visser J A G M and Krug J 2011 *PLoS Comput Biol* **7** e1002134
- [43] Nowak S and Krug J 2013 *EPL (Europhysics Letters)* **101** 66004
- [44] Aita T, Uchiyama H, Inaoka T, Nakajima M, Kokubo T and Husimi Y 2000 *Biopolymers* **54** 64–79
- [45] Neidhart J, Szendro I G and Krug J 2014 *Genetics* **198** 699–721
- [46] Weinberger E D 1991 *Phys. Rev. A* **44** 6399–6413
- [47] Stadler P 1996 *Journal of Mathematical Chemistry* **20** 1–45
- [48] Weinberger E 1991 *Biological Cybernetics* **65** 321–330
- [49] Weinreich D M, Lan Y, Wylie C S and Heckendorn R B 2013 *Current Opinion in Genetics & Development* **23** 700–707
- [50] Gillespie J H 1983 *The American Naturalist* **121** 691–708
- [51] Orr H A 1998 *Evolution* **52** 935–949
- [52] Neidhart J and Krug J 2011 *Phys. Rev. Lett.* **107** 178102
- [53] Jain K 2011 *EPL (Europhysics Letters)* **96** 58006

- [54] Seetharaman S and Jain K 2014 *Evolution* **68** 965–975
- [55] Contucci P, Giardina C, Giberti C, Unguendoli F and Vernia C 2005 *Optimization Methods and Software* **20** 509–514
- [56] Contucci P, Giardina C, Giberti C and Vernia C 2005 *Mathematical Models and Methods in Applied Sciences* **15** 1349–1369
- [57] Bussolari L, Contucci P, Esposti M D and Giardina C 2003 *Journal of Physics A: Mathematical and General* **36** 2413–2421
- [58] Valente M 2014 *Journal of Evolutionary Economics* **24** 107–134
- [59] Macken C A and Perelson A S 1989 *Proceedings of the National Academy of Sciences* **86** 6191–6195
- [60] Macken C A, Hagan P S and Perelson A S 1991 *SIAM Journal on Applied Mathematics* **51** 799–827
- [61] Flyvbjerg H and Lautrup B 1992 *Phys. Rev. A* **46** 6714–6723
- [62] Orr H A 2003 *Journal of Theoretical Biology* **220** 241 – 247
- [63] de Haan L and Ferreira A 2006 *Extreme Value Theory: An Introduction* (New York: Springer)
- [64] Baldi P and Rinott Y 1989 *Journal of Applied Probability* **26** 171–175
- [65] Østman B and Adami C 2014 Predicting evolution and visualizing high-dimensional fitness landscapes. *Recent Advances in the Theory and Application of Fitness Landscapes (Emergence, Complexity and Computation vol 6)* pp 509–526
- [66] Manukyan N, Eppstein M J and Buzas J S 2014 (*Preprint arXiv:1409.1143*)
- [67] Kouyos R D, Leventhal G E, Hinkley T, Haddad M, Whitcomb J M, Petropoulos C J and Bonhoeffer S 2012 *PLoS Genet.* **8** e100255151
- [68] Balkema A A and de Haan L 1974 *The Annals of Probability* **2** 792–804
- [69] Pickands III J *The Annals of Statistics* **3** 119–131